

Maria Gabriela Louzada Malfatti¹ (mglmalfatti@usp.br); Lucas Massarope²; Pedro Leite da Silva Dias²

¹Institute of Energy and Environment, University of São Paulo; ²Institute of Astronomy, Geophysics and Atmospheric Sciences, University of São Paulo.

INTRODUCTION

- In meteorology, identification of teleconnections between climatic phenomena plays an important role in the validation of atmospheric models which are used for weather and climate prediction and for the development of future climate scenarios.
- In order to evaluate the connectivity between climatic phenomena, correlation analysis is often used, but this type of analysis may lead to oversimplified relationships, which does not imply causality between different scales of time.
- In this work, Partial Directed Coherence (PDC) and kernel non-linear Partial Directed Coherence (*kn*PDC) were used to infer the influence between atmospheric compartments (atmosphere and ocean), allowing the detection of linear and non-linear connections, respectively, between variables representative of important climatic variability modes.

DATA AND METHODOLOGY

Climate Indices (1950 to 2018)

National Oceanic and Atmospheric Administration (NOAA)
PSA index: defined by the 2nd (PSA1) and 3rd (PSA2) EOF of the monthly mean 500hPa geopotential anomalies (Mo, 2000).

Groups of climatic indicators

El Niño-Southern Oscillation (ENSO); Atlantic Multidecadal Oscillation (AMO); Pacific Decadal Oscillation (PDO); Atlantic Interhemispheric SST Gradient (GTA)

Antarctic Oscillation (AAO); Pacific Decadal Oscillation (PDO); Pacific-South American (PSA1 and PSA2)

Inference of the linear or nonlinear couplings between the climatological patterns

Partial Directed Coherence (PDC) [1]

Nonlinear Partial Directed Coherence kernel (*kn*PDC) [2]

We represent the input series $\{x_i(n)\}_{n=1}^N$ (input space) through a Kernel Vector Autoregressive (kVAR) model, such as in (Massarope and Baccalá, 2019)

$$\langle \phi(x(n)) \rangle = \sum_{r=1}^p A_k \langle \phi(x(n-k)) \rangle + \langle \tilde{w}(n) \rangle,$$

where

- $\{\langle \tilde{w}(n) \rangle\}_{n \in \mathbb{Z}} \sim i.i.d. WN(0, \Sigma_{\langle \tilde{w}(n) \rangle})$
- $\phi: \mathbb{X} \rightarrow \mathbb{F}$ represents a nonlinear mapping (Parzen, 1959), such that $\mathbb{E}\{\langle \phi[x_i(n)] \rangle \langle \phi[x_i(n-k)] \rangle\} = \mathbb{E}\{x_i(n) x_i(n-k)\}$;
- $\kappa(\cdot)$: a Mercer kernel;
- $\langle \cdot | \cdot \rangle$: Dirac's 'bracket' notation.

The *kernel-nonlinear*-Partial Directed Coherence is defined, in the phase space, as

$$\kappa \eta \pi_{ij}(f) = \frac{\bar{A}_{ij}(f) / \sqrt{\sigma_{ii}}}{\sqrt{\bar{a}_{jj}(f) \Sigma_{\langle \tilde{w}(n) \rangle}^{-1} \bar{a}_{jj}(f)}}$$

where

- $\bar{A}_{ij}(f) = \delta_{ij} - \sum_{r=1}^p a_{ij}^{\phi}(r) e^{-i2\pi f r}, (i^2 = -1)$;
- $a_{ij}^{\phi}(r)$ are the coefficients of an adequately adjusted *k*VAR model;
- $\bar{a}_j(f)$ represent the columns of the $[\bar{A}_{ij}^{\phi}(f)]$ matrix.

PDC is similarly defined and can be seen in (Baccalá et al., 2013).

RESULTS

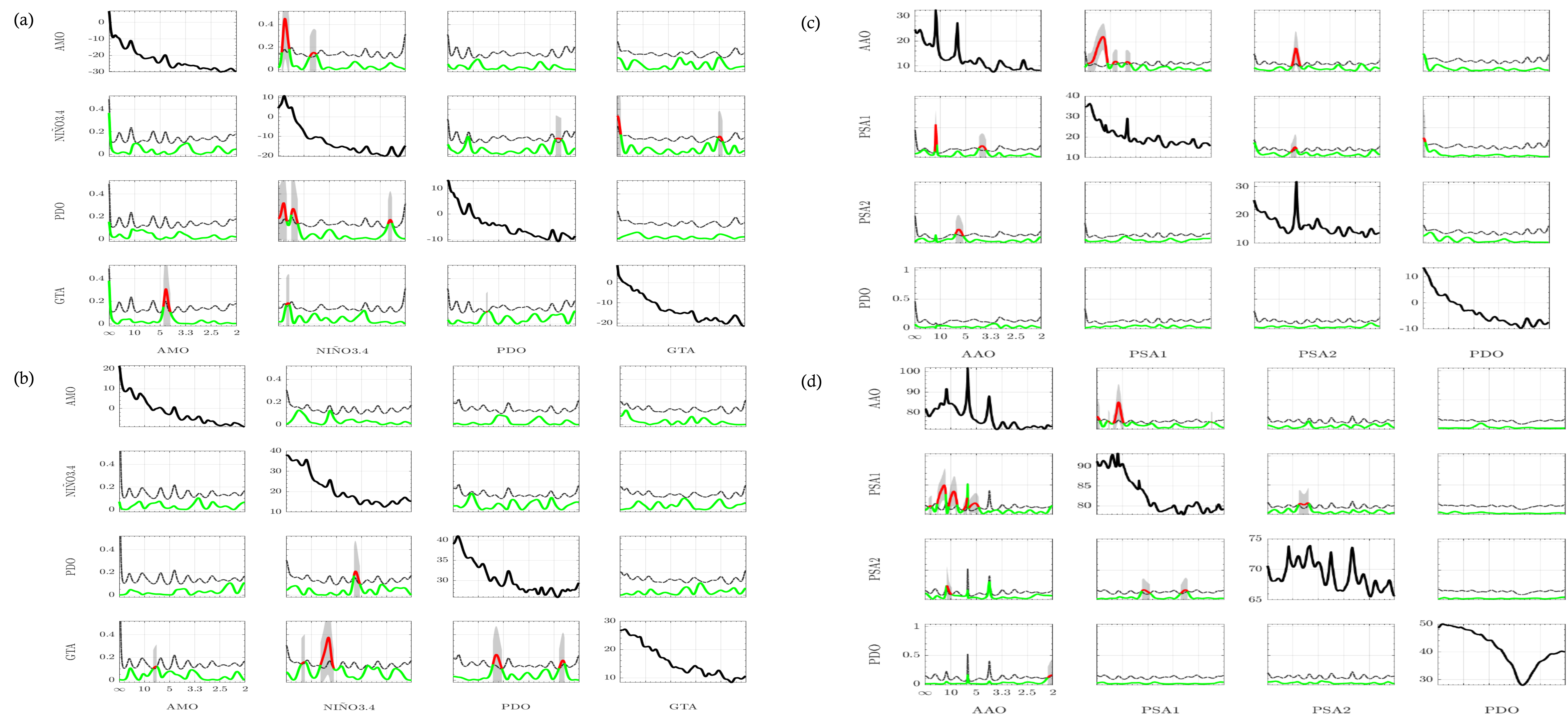


Fig. 1. The black plot represents the (pseudo-) spectral density of the series in dB; the red line represents the statistically significant PDC / *kn*PDC values; the dashed black line represents Patnaik's threshold approximation (Baccalá et al., 2013); the green line the statistically non-significant PDC / *kn*PDC values. Therefore, using 1% significance level, the figures depict, respectively: (a) PDC for time series set (AMO, Niño 3.4, PDO and GTA) using an autoregressive model of order $p = 48$, (b) *kn*PDC for the time series set (AMO, Niño 3.4, PDO and GTA), using the polynomial kernel $[k(x, y) = (x \cdot y)^2]$ and using a *kernel*-autoregressive model of order $p = 24$, (c) *kn*PDC for the time series set (AAO, PSA1, PSA2 and PDO) and using an autoregressive model of order $p = 48$, (d) *kn*PDC for the time series set (AAO, PSA1, PSA2 and PDO) and using the polynomial kernel $[k(x, y) = (x \cdot y)^2]$ and using a *kernel*-autoregressive model of order $p = 24$.

It is observed that ENSO influences all other analyzed climate variability patterns (AMO, PDO and GTA) as indicated in other studies concerning extratropical teleconnections between Atlantic and Pacific oceans, where ENSO exerts greater influence on the North Atlantic (Rodríguez-Fonseca et al., 2016; García-Serrano et al., 2017). Similar studies have observed the causal relationship between the Pacific (Niño 3) and the Atlantic (TNA) (Builes-Jaramillo et al., 2018). In addition, Fig. 1b also shows that PDO has a nonlinear causal relationship with GTA, evidencing that the Pacific exerts influence in the Atlantic.

Furthermore, the results obtained by PDC and *kn*PDC suggest that SO also causes PDO and are related linearly (Fig. 1a) and nonlinearly (Fig. 1b). Theoretical studies (Ramirez et al., 2017) also support this conclusion from a theoretical point of view.

The results also indicate to linear and nonlinear relationships between $AAO \leftarrow \rightarrow PSA1$ and $AAO \leftarrow \rightarrow PSA2$. The *kn*PDC analysis also indicates causality between PDO and AAO in agreement with some studies that suggest the influence of PDO on AAO in summer and late winter (Pezza et al., 2007; Goodwin et al., 2016).

DISCUSSION AND CONCLUSIONS

The causality analysis suggests that ENSO causes AMO and AITG causes PDO, highlighting the non-linear relations $ENSO \rightarrow PDO$ and $ENSO \rightarrow AITG$. Furthermore, we observe the influences $PDO \rightarrow AITG$ and $PDO \rightarrow AAO$, evidencing the energy transfer from the Pacific to the Atlantic Ocean. In addition, PDC and *kn*PDC techniques results suggest that some indices have non-linear interaction, emphasizing the use of non-linear machine learning techniques, e.g., deep learning, that are able to capture these variations.

ACKNOWLEDGMENTS

The authors gratefully acknowledge support from the FAPESP Grant 2015/50686-1 (PACMEDY Project). M.G.L.M. to CNPq Grant 2017/05285-4 (Ph.D. Scholarship). L.M. to CAPES Grant 88887.161474/2017-00 (PALEOCEANO Project).

REFERENCES

- [1] MO, K. C. Relationship between Low-Frequency Variability in the Southern Hemisphere and Sea Surface Temperature Anomalies. **J. Clim.**, v. 13, p. 3599-3610, 2000.
- [2] PARZEN, E. Statistical inference on time series by Hilbert space method, I. Technical Report 23, Applied Mathematics and Statistics Laboratory, Stanford University, Stanford, January 1959.
- [3] MASSAROPPE, L. and BACCALÁ, L. A. Kernel methods for nonlinear connectivity detection. **Entropy**, 2019.
- [4] BACCALÁ, L. A. et al. Unified asymptotic theory for all partial directed coherence forms. **Philosophical Transactions of the Royal Society A: Mathematical, Physical and Engineering Sciences**, v. 371, n. 1997, p. 20120158, 2013.
- [5] RODRÍGUEZ-FONSECA et al., A review of ENSO influence on the North Atlantic. A Non-Stationary Signal. **Atmosphere**, v. 7 n. 7, 87, 2016.
- [6] GARCÍA-SERRANO et al., Revisiting the ENSO teleconnection to the Tropical North Atlantic. **Journal of Climate**, v. 30, n. 17, p. 6945-6957, 2017.
- [7] BUILES-JARAMILLO, A.; RAMOS, A. M. T.; POVEDA, G. Atmosphere-Land Bridge between the Pacific and Tropical North Atlantic SST's through the Amazon River basin during the 2005 and 2010 droughts. **Chaos**, v. 28, 085702, 2018.
- [8] RAMIREZ, E.; SILVA DIAS, P. L.; RAUPP, C. F. M. Multiscale atmosphere-ocean interactions and the low-frequency variability in the Equatorial region. **Journal of the Atmospheric Sciences**, v. 74, n. 8, p. 2503-2523, 2017.